Title: A head-fixation system for continuous monitoring of force generated during behavior

Authors: Ryan N. Hughes[1], Konstantin I. Bakhurin[1], Joseph W. Barter[1], Jinyong Zhang[1], Henry H. Yin[1,2]

Affiliations:

[1]Department of Psychology and Neuroscience, Duke University, Durham, NC, 27708, USA.,

[2]Department of Neurobiology, Duke University School of Medicine, Durham, NC, 27708, USA.

Correspondence to: **hy43@duke.edu**

Abstract

Many studies in neuroscience use a head-fixed preparation for performing well-controlled behavioral experiments. While head fixation confers a number of advantages, including the ability to limit the behavioral repertoire and use techniques for large-scale monitoring of neural activity, traditional studies suffer from a number of limitations. It is often assumed that, other than the behavioral variables of interest to the experimenter, no other behaviors occur. This is primarily because it is difficult to detect subtle movements and postural adjustments. Here we report the development of a head-fixation apparatus that is equipped with load cells capable of monitoring the continuous forces exerted by mice. The apparatus reveals the dynamic nature of movements that are continuously generated by animals during the presentation of highly stereotyped stimuli and rewards, and even during periods of no apparent overt behavior. It generates a new set of behavioral measures neglected in previous experiments. We detail the construction of the device, which can be 3D-printed at low cost. We also show behavioral results collected from head-fixed mice and demonstrate that neural activity is highly correlated with subtle whole-body movements during head fixation.

Introduction

Many studies in modern behavioral neuroscience use head-fixation (Coddington & Dudman, 2018; Economo et al., 2018; Toda et al., 2017). Historically, head-fixed experimental preparations in awake behaving animals have contributed to the study of motor control (Evarts, 1968; Hikosaka & Wurtz, 1983), associative learning(Eshel et al., 2015; Waelti, Dickinson, & Schultz, 2001), and even navigation (Dombeck, Harvey, Tian, Looger, & Tank, 2010). Head-fixation confers two major advantages. First, it allows convenient monitoring of neural activity that minimizes noise and motion artifact. This enables the use of powerful techniques for recording neural activity on a large scale, such as two-photon calcium imaging or electrophysiology using large electrode arrays. Second, by greatly constraining the behaviors that the animal can perform, it simplifies experimental design and data analysis. For this reason, studies using head-fixation usually constrain their focus to the behavior of interest. These measures are usually restricted to licking, EMG measures of arm or mouth muscle activity, bar pressing, or eye movements(Economo et al., 2018; Eshel et al., 2015; Newsome, Britten, & Movshon, 1989; Schultz, Apicella, Scarnati, & Ljungberg, 1992). While these measurements have provided valuable insights, other behaviors generated by the head-fixed animals are neglected. Many postural adjustments of the body are not measured. Additionally, it is often assumed that no other behaviors, such as head movements, are occurring because overt movements cannot be easily observed. However, it does not follow that there are not muscular contractions or attempts to move the head. Furthermore, often the animals are placed in chambers or rooms away from the experimenter, so that close observation of the actual behavior is not even possible. Because neural activity recorded during standard behavioral tasks could well be related to the generation of such movements, they produce significant confounding

variables. The lack of knowledge of such variables can therefore result in misinterpretation of neural activity, while the true relationship between neural activity and behavior is overlooked.

More recent head-fixation systems have attempted to address some of these concerns by incorporating a running ball beneath animals' feet (Dombeck et al., 2010; Engelhard et al., 2019). During such experiments, animals often make direction-specific adjustments of the body and the head, in addition to their limb movements, in order to steer the ball appropriately. However, the coordinate (x, y, and z) positions of the ball provide little information about the actual kinematics of the body. How animals exert torques and forces at the head-fixation point to steer the ball during these tasks has never been measured.

Others have incorporated accelerometers into their head-fixation devices, thus allowing for measurements of whole-body movements (Coddington & Dudman, 2018). The biggest limitation to accelerometer baskets is they cannot distinguish between movements in different directions, as movements in any direction can result in the same accelerometer reading. Importantly, such approaches also fail to measure the movements made by the head.

Here we describe a novel head-fixation apparatus equipped with load cells for detection of force generated by head-fixed mice. The apparatus reveals the dynamic nature of movements that are continuously generated by head-fixed animals during behavior.

Results

To measure movement and movement intention accurately in head-fixed approaches, we developed a novel head-fixation device that incorporates 5 load cells to directly measure the forces generated by the mice's head and body movements (Figure 1A). Animals are implanted

with a steel head post as part of routine surgery to implant electrodes into the brain. The post is secured into the apparatus by small pinch clamps, which are part of a lightweight, rectangular plastic frame. The height of the frame was determined by the need to accommodate neural recording hardware installed onto the electrode array. The frame is suspended by an array of 3 aluminum load cells that are arranged orthogonally (Figure 1).

The precise arrangements of the load cells enabled the measurement of independent force vectors along orthogonal axes of movement (up/down, left/right, or forward/backward). The load-cells are arranged in a tight cluster together immediately above the animal to avoid spurious measures of torque as well as to capture as much of the individual force vector as possible. Two additional sensors were placed below the animals' feet in a custom-designed perch (Figure 1B). These sensors reflect the forces exerted by each side of the body through the feet as the animal moves the head and adjusts its posture. All components of the head-fixation device were custom-designed and 3-D printed in the lab.

Small strain gauge load cells designed to operate on a scale of 0-100g were used. Load cells of this type and size are most commonly found in small weighing devices such as kitchen and coffee scales. Attached to the aluminum body of the load-cell are sensitive strain gauges arranged in a whetstone bridge configuration (Figure 2A). Changes in the shape of the bridge alters its resistance and affects voltage levels across the gauges. Because the load-cells register changes to the shape of their aluminum bodies, the cluster of 3 load cells that support the head-fixation frame acts as the frame's pivot-point as it slightly moves along 3-dimensions in response to the animal's movement. Current through the load cell is modulated by deformations of the strain gauges, which can be detected as small changes in voltage that are proportional to the amount of force exerted. The load cell is coupled to an amplifier circuit that that scales this

voltage between 0 and 5V, which can be used by most analog recording systems (Figure 2A). The configuration of the circuit shown is designed to detect bidirectional forces exerted on the load cell. Using a low-resistance trim potentiometer between pins 8 and 9 in the amplification circuit allows the user to adjust the gain to make maximum use of the data acquisition system's resolution (Figure 2B). The load cell signal is linearly proportional to the amount of force applied to it. By measuring the slope between known masses and the voltage reading, it is possible to convert the measured voltage to force applied to the load cell by the animals.

Behavior on a fixed-time reinforcement schedule

In order to test our load-cell head-fixation device, we trained 2 mice on a fixed-time schedule of reinforcement where they received a 10% sucrose solution every 10 seconds (Figure 3A). The mice exhibited fine and subtle movements as they engaged in the task (Figure 3). The signals registered by each load cell were distinct for a given trial, reflecting the complexity of coordinated movements generated by different parts of the body. The animals' force exertion was often coincident their licking for reward. In mice licking is stereotyped (Rossi et al., 2016; Rossi & Yin, 2015; Toda et al., 2017). The high frequency oscillations that result from licking could be detected in the force sensors (Figures 3B-K). Licking related oscillations were nested within slower-frequency movements that reflected positional and postural changes of the whole body. Movements were typically seen in all 5 orthogonal force sensors with distinct changes of amplitude and direction (Figures 3B-K).

The dynamic force signals detected by the load-cells reflect subtle changes in movement of the head and posture of the body that vary from one trial to another. We therefore asked

whether such continuous measures of movement are related to neural activity. Neurons in the VTA have recently been demonstrated to control the angular position of the head in three-dimensional space(Hughes et al., 2019). To determine whether VTA activity is related to forces in the head-fixation system, we recorded single unit activity from the VTA during the fixed-time task (n = 2, Figure 4A).

Force signals that we measured frequently coincided with licking. By aligning and neural activity to reward and sorting all recorded data by the latency to lick relative to reward, we can reveal striking patterns among behavioral variables (Figure 4B). The raster plots and heat maps of continuously measured kinematic variables show high trial-to-trial variability. By extension, neural data aligned in the same manner showed organized force and movement-dependent activity (Figure 4H). We found similar examples in a second animal with VTA recordings (Figures 4I-O).

Behavior during Pavlovian conditioning

We also recorded VTA activity from two different mice on a Pavlovian trace conditioning task (Figure 5A). During this task, a 100 ms tone (CS) was presented at random intervals followed by a 1 second delay. After the delay period, a 10% sucrose solution was delivered (US). We simultaneously recorded their neural activity and force exerted during this task (Figures 5B & 5D). The mice would typically exert the most force immediately following reward delivery (Figure5C & 5E). Significantly, the neural activity often closely followed these force changes (Figures 5B-E). Thus, these preliminary results our experimental setup

demonstrates that there are valuable behavioral measurements besides licking that can be taken during Pavlovian conditioning tasks.

Discussion

One major limitation in behavioral neuroscience research is the lack of precise, continuous and direction-specific behavioral measurements, especially when animals are head-fixed. Even though the animal is fixed in place, it is often making many continuous adjustments of the head and body while performing a given task. But these behaviors are conveniently neglected in traditional neuroscience experiments.

Although head-fixation allows for the more precise monitoring of various behaviors of interest, such as licking, our device shows that there are many movements that can be correlated with those measures, even though they are never measured. In addition, the strain on the skull resulting from movements generated while clamped to a rigid structure presents an unavoidable source of variable sensory input for the nervous system. Therefore, two major confounds exist in many previous studies using head-fixed approaches while investigating the neural substrates of behavior.

One possible reason this has not been taken seriously is that the traditional approach is based on experimenter-defined behavioral events. Actions are often assumed to be 'all-or-none' discrete events, such as reaching, licking, button pressing, or saccades. Behavior is thus only quantified as a categorical time stamp, rather than as a continuous process which unfolds over time. As a result, investigators have only attempted to understand neural activity by aligning it to this observer-defined action and analyzing its activity around this time point. Even a behavior as

simple as eating a piece of food entails coordinating multiple muscle effectors with a variety of perceptual variables (e.g. jaw, arm and tongue muscles being coordinated in relation to the distance of the piece of food to the mouth). The time courses and dynamics of these variables would also be distinct for every individual piece eaten. Our force measures demonstrate that mice make many head and body movements during traditional head-fixation studies, and their neural activity can reflect these behavioral changes (Figures 3-5). Thus, many studies claiming to investigate the neural correlates of variables such as reward or value during head-fixed studies have failed to notice this movement confound. It would be helpful to investigate all previous head-fixed experiments using continuous force measures as introduced here.

Variability in neural activity has long been a puzzle in neuroscience (Osborne, Lisberger, & Bialek, 2005; Shadlen & Newsome, 1998). The results obtained from our novel head-fixation device point towards a potential source of this variability: continuous behavior that has not been noticed or measured. By aligning the force measures and neural activity to experimenter-defined events, the neural activity outside of these events (which has traditionally been regarded as noise or unimportant) can be seen to reflect the continuous force measures. This immediately reveals a potential source of the 'noise' in nervous system activity (Figures 4 and 5). These results should not be viewed as noise but as data to be explained by any theory of the brain.

Our head-fixation set-up addresses these problems by continuously measuring the forces exerted by the animal's head as well as the forces exerted by both sides of the body. The chief advantages of our head-fixed design are its low-cost, ease of construction, and its precise, direction-specific measurements of the mice's head and body.

While newer head-fixed set ups utilize a running ball or an accelerometer in order to measure the behavior of the animal, there are several disadvantages associated with these

setups(Coddington & Dudman, 2018; Harvey, Collman, Dombeck, & Tank, 2009). First, it is impossible to detect direction-specific adjustments of the head and body with either an accelerometer basket or a running ball. Second, the coordinates and the speed of the ball are only indirect measures of the actual kinematics of the mice. These measurements do not provide accurate representations of the animal's kinematics or dynamics. Furthermore, the treadmill ball has its own momentum that can be in conflict with how the mice are moving. In other words, if the ball is moving to the left, but the mice want to go forward, many opposing adjustments of the limbs and body have to occur to counteract the balls momentum for the mice to go straight. The measures from the ball could indicate a turn from left to forward whereas the mice are making large adjustments in different directions in order to obtain the new heading.

Our head-fixation system can be used in conjunction with treadmills balls to detect these adjustments, where the direction-specific head movements can be measured and directly compared with the coordinates obtained from the ball. This would make it possible to dissociate head movements and limb movements.

To further our understanding of how the nervous system is coordinating these highly variable and rich movements, behavior must be continuously measured with temporal precision and direction-specificity. Only then can behavior be adequately related to the corresponding neural activity (Figures 4-5).

Methods

Animals. All experimental procedures were approved by the Animal Care and Use Committee at Duke University. Four C57BL/6J mice between 2-6 months old were used for experiments

(Jackson Labs, Bar Harbor, ME). Mice were housed in groups of 3-4 animals per cage on a 12:12 light cycle, with experiments conducted during the light phase. During days where mice were run on experiments, they were water restricted and maintained at 85-90% of their initial body weights. Animals received free access to water for approximately 2 hours following the daily experimental session.

Load Cells and Circuit: Each load cell (RobotShop, Swanton, VT, USA) is a full Wheatstone bridge with a configuration of four balanced resistors based on a known excitation voltage, as shown below:

$$V_f=(R_3R_3+R_4-R_2R_1+R_2)V_{EX}$$

Where R is the resistor, V_{EX} is a known constant excitation voltage, and output V_f is variable depending on the shape of the strain gauge. Thus, a bidirectional sensing amplifier connected to the load cell will output 2.5V at zero load. When the load is increased or decreased, the voltage will correspondingly increase or decrease. In other words, if the load is positive, voltage output will increase, and if the load is negative, voltage will decrease. This relationship is described by the following:

$$V_f=2.5V+G_f\cdot k\cdot F_a$$

Where G_f is the amplifier's gain, k is the cell sensitivity and F_a is the force applied to the load cell. We also attached a trim potentiometer to the circuit. The sensitivity of the circuit can be adjusted using the potentiometer, which is a precise trimmer potentiometer with 100 Ohms resistance. We used a high accuracy amplifier (INA125, Texas Instruments) chip, which has a precision voltage reference. The amplifier gain (Gf) from this chip is described as below.

G_f=4+60k/R_g

Where Rg is the resistance of the potentiometer.

The voltage obtained from the amplifier (INA125) is then linearly correlated with the force on the load cell. That means we can use the voltage to describe the force exerted on each orthogonal load cell. From Newton's second law ($F = ma$, where F = force, m = mass and a = acceleration), a mass with a known quantity placed on the load cell can be multiplied by gravity in order to obtain a force-voltage conversion factor (F/V). This conversion factor can then be used to convert the voltage signal to a force that is being exerted on the load cell.

Head-fixed behavioral setup. A novel mouse perch and adjustable head-fixation apparatus were designed and 3D printed in PLA plastic using a MakerGear M2 3D printer (MakerGear, Beachwood, OH, USA). Both mouse perch and head fixation apparatus were bolted to a steel base plate (Thorlabs, Newton, NJ, USA), and elevated to give sufficient space for the reward delivery apparatus. In the floor of the perch, two 100g load cells (RobotShop, Swanton, VT, USA) were used to measure ground reaction forces on the left and right side of the mice. The mice's head implants were clamped to a custom frame that was suspended above them. In the head fixation apparatus between the point of head fixation and the base plate, three 100g load cells of the same type were arranged orthogonally to detect force changes in three dimensions (forwards-backwards, up-down, and left-right). These load cells were connected in series and arranged close together and in line with the animal's head to minimize twisting forces. Each load cell was connected by a shielded cable to an amplifier circuit, which was in turn connected to the data acquisition system. Each load cell signal was recorded continuously as an analog voltage.

Load cells translate mechanical stress caused by an applied load into a voltage signal. We amplified the signal using an INA125P (Texas Instruments; http://www.mechtechplace.net/mech-tech-electronics/building-a-low-cost-strain-gage-load-cell-amplifier/). A 10 % sucrose solution gravity-fed from a reservoir was delivered to the mice via a metal spout placed in close proximity to their mouth. Sucrose delivery was controlled through the use of a solenoid valve (161T010, NResearch, NJ). A capacitance-touch sensor (MPR121, AdaFruit.com) was clamped to the metal spout in order to record licking behavior. All analog voltage signals (1 Khz) and electrophysiological data were recorded using a Blackrock Cerebrus recording system (Blackrock Microsystems) for offline analysis.

Wireless *in Vivo* Electrophysiology:

Mice were anesthetized with 2.0 to 3.0% isoflurane, then placed into a stereotactic frame (David Kopf Instruments, Tujunga, CA) that was maintained at 1.0 to 1.5 % isoflurane for surgical procedures, as previously described(Fan et al., 2011; Fan, Rossi, & Yin, 2012). A craniotomy was then made above the VTA. Fixed 16-channel electrodes (Innovative Neurophysiology, Inc.) were lowered into the VTA (AP: 3.2 mm, ML 0.5 mm, DV, -4.2 mm) through the craniotomy. Electrode arrays were composed of tungsten electrodes in a 4 x 4 configuration (35 µm diameter, 150 µm spacing, 5 mm length). After electrodes were inserted, they were secured to the skull using screws and dental acrylic, followed by the insertion of a metal bar around the dental acrylic to allow for head-fixation (Toda et al., 2017). Mice were allowed to recover for 2 weeks, then trained on the fixed time reinforcement schedule for approximately 1 week until clear anticipatory licking was observed. A miniaturized wireless head stage (Triangle Biosystems) that communicated with a Cerebrus data acquisition system (Blackrock Microsystems) was used to

record electrophysiological data (Barter et al., 2015; Fan et al., 2011). All single unit data were then sorted offline using OfflineSorter (Plexon). All plots for electrophysiological and force signal data were created with NeuroExplorer (Nex Technologies) using 50 ms timebins. In order to be included for analysis, neural data must have had a 3:1 signal-to-noise ratio, with an 800 μs or greater refractory period.

Figure legends

Fig. 1. **Novel head-fixation set up measures force of the head in 3 orthogonal directions and eft and right body forces**

A) Illustration of novel head-fixation apparatus with five orthogonal force sensors. There are three force sensors that measure the force exerted by the mice's head (1, 2 and 3). Two additional force sensors are below the mice's feet on the left and right side of the body (4 and 5). **B**) Schematic representation of each force sensors and the direction of force that it measures. Force sensor 1 measures force made by the head in the forwards and backwards direction. Force sensor 2 measures force made by the head in the side-to-side (left and right) direction. Force sensor 3 measures force made by the head in the upward and downward direction. Force sensors 4 and 5 measure force exerted in the upward and downward direction made by the right and left feet, respectively

Fig. 2. **Load cell circuit and set up allows for data acquisition with any device that can read an analog signal**

A) Circuit diagram for the load cell. The load cell is attached to an amplifier which also contained a potentiometer that allows the user to change the resistance of the load cell in order to tune it for optimal linear relationship between voltage and the force applied to the load cell. From this circuit, the voltage output is then connected to a data acquisition system to collect continuous voltage signal data. **B**) There is a linear relationship between mass applied to the load cell and the change in voltage output. By using an object with a known mass, a mass-voltage

relationship can be obtained using different levels of resistance from the potentiometer. From Newton's second law ($F = ma$), the known mass can be multiplied by gravity in order to obtain a force-voltage conversion factor (F/V) in order to obtain the force exerted on the load cell.

Fig. 3. **Force sensors detect continuous and fine movements of the head and body in a fixed time behavioral task**

A) Two mice were trained on a fixed-time schedule of reinforcement where they received a 10% sucrose solution every 10 seconds. **B-F)** Raw continuous traces of 10 seconds from all five force sensors, as well as lick times, obtained from mouse 1. Each force sensor displays distinct force changes that vary in their amplitude and direction. **G-H)** Raw continuous traces of 10 seconds from all five force sensors, as well as lick times, obtained from mouse 2.

Fig. 4. **Neural data and precise force measurements can be used to find relationships between neural activity and behavior in head-fixed set ups.**

A) An electrode was implanted into the VTA (n = 2). Waveform of typical putative VTA GABAergic neuron shown on right. **B**) Representative putative GABAergic neuron aligned to the onset of licks after reward from mouse 1. Trials were sorted according to the initiation of the first lick. **C**) Corresponding licks from the same behavioral session. **D-H)** Data from all 5 force sensors aligned to the onset of licks after reward (mouse 1). **I**) Representative putative GABAergic neuron aligned to the onset of licks after reward from mouse 2. **J**) Corresponding

licks from the same behavioral session. **K-O)** Data from all 5 force sensors aligned to the onset of licks after reward (mouse 2).

Fig. 5. **Characteristic force measures and neural activity on a Pavlovian conditioning task.**

A) Mice were trained on a Pavlovian trace conditioning task where a 100 ms tone (CS) was presented, followed by a 1 second delay and the delivery of a 10 % sucrose reward (US). There was a random interval trial interval (ITI) of 3-60 seconds. **B)** Two representative putative GABAergic neurons from the VTA of mouse 3. Trials are sorted according to the start of the first forward movement. **C)** Corresponding head force measures showing mice exert large head forces during the task. **D)** Two representative putative GABAergic neurons from the VTA of mouse 4. Trials are sorted according to the start of the first forward movement. **E)** Corresponding head force measures during the task.

Barter, J. W., Li, S., Sukharnikova, T., Rossi, M. A., Bartholomew, R. A., & Yin, H. H. (2015). Basal ganglia outputs map instantaneous position coordinates during behavior. *Journal of Neuroscience, 35*(6), 2703–2716.

Coddington, L. T., & Dudman, J. T. (2018). The timing of action determines reward prediction signals in identified midbrain dopamine neurons. *Nat Neurosci, 21*(11), 1563.

Dombeck, D. A., Harvey, C. D., Tian, L., Looger, L. L., & Tank, D. W. (2010). Functional imaging of hippocampal place cells at cellular resolution during virtual navigation. *Nat Neurosci, 13*(11), 1433-1440. doi:10.1038/nn.2648

Economo, M. N., Viswanathan, S., Tasic, B., Bas, E., Winnubst, J., Menon, V., . . . Svoboda, K. (2018). Distinct descending motor cortex pathways and their roles in movement. *Nature, 563*(7729), 79-84. doi:10.1038/s41586-018-0642-9

Engelhard, B., Finkelstein, J., Cox, J., Fleming, W., Jang, H. J., Ornelas, S., . . . Witten, I. B. (2019). Specialized coding of sensory, motor and cognitive variables in VTA dopamine neurons. *Nature*, 1.

Eshel, N., Bukwich, M., Rao, V., Hemmelder, V., Tian, J., & Uchida, N. (2015). Arithmetic and local circuitry underlying dopamine prediction errors. *Nature, 525*(7568), 243-246. doi:10.1038/nature14855

Evarts, E. V. (1968). Relation of pyramidal tract activity to force exerted during voluntary movement. *J Neurophysiol, 31*(1), 14-27.

Fan, D., Rich, D., Holtzman, T., Ruther, P., Dalley, J. W., Lopez, A., . . . Yin, H. H. (2011). A wireless multi-channel recording system for freely behaving mice and rats. *PloS one, 6*(7), e22033. doi:10.1371/journal.pone.0022033

Fan, D., Rossi, M. A., & Yin, H. H. (2012). Mechanisms of action selection and timing in substantia nigra neurons. *J Neurosci, 32*(16), 5534-5548. doi:32/16/5534 [pii]

Harvey, C. D., Collman, F., Dombeck, D. A., & Tank, D. W. (2009). Intracellular dynamics of hippocampal place cells during virtual navigation. *Nature, 461*(7266), 941-946. doi:10.1038/nature08499

Hikosaka, O., & Wurtz, R. H. (1983). Visual and oculomotor functions of monkey substantia nigra pars reticulata. III. Memory-contingent visual and saccade responses. *J Neurophysiol, 49*(5), 1268-1284.

Hughes, R. N., Watson, G. D., Petter, E. A., Kim, N., Bakhurin, K. I., & Yin, H. H. (2019). Precise Coordination of Three-Dimensional Rotational Kinematics by Ventral Tegmental Area GABAergic Neurons. *Current Biology*.

Newsome, W. T., Britten, K. H., & Movshon, J. A. (1989). Neuronal correlates of a perceptual decision. *Nature, 341*(6237), 52-54. doi:10.1038/341052a0

Osborne, L. C., Lisberger, S. G., & Bialek, W. (2005). A sensory source for motor variation. *Nature, 437*(7057), 412-416.

Rossi, M. A., Li, H. E., Lu, D., Kim, I. H., Bartholomew, R. A., Gaidis, E., . . . Yin, H. H. (2016). A GABAergic nigrotectal pathway for coordination of drinking behavior. *Nat Neurosci*. doi:10.1038/nn.4285

Rossi, M. A., & Yin, H. H. (2015). Elevated dopamine alters consummatory pattern generation and increases behavioral variability during learning. *Front Integr Neurosci, 9*, 37. doi:10.3389/fnint.2015.00037

Schultz, W., Apicella, P., Scarnati, E., & Ljungberg, T. (1992). Neuronal activity in monkey ventral striatum related to the expectation of reward. *J Neurosci, 12*(12), 4595-4610.

Shadlen, M. N., & Newsome, W. T. (1998). The variable discharge of cortical neurons: implications for connectivity, computation, and information coding. *J Neurosci, 18*(10), 3870-3896.

Toda, K., Lusk, N. A., Watson, G. D. R., Kim, N., Lu, D., Li, H. E., . . . Yin, H. H. (2017). Nigrotectal Stimulation Stops Interval Timing in Mice. *Curr Biol, 27*(24), 3763-3770 e3763. doi:10.1016/j.cub.2017.11.003

Waelti, P., Dickinson, A., & Schultz, W. (2001). Dopamine responses comply with basic assumptions of formal learning theory. *Nature, 412*(6842), 43-48.

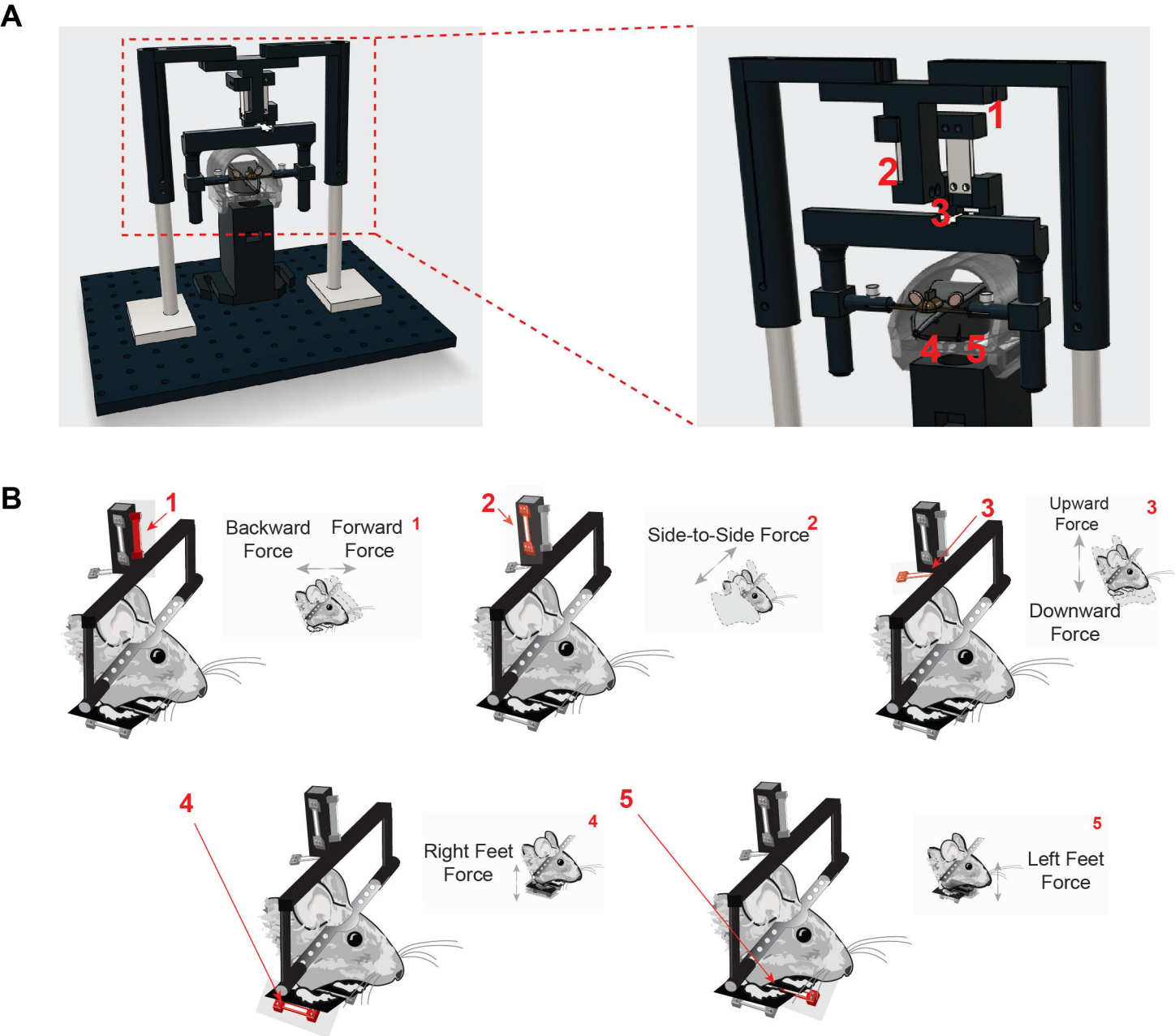
A
1
2
3
4
5
B
1
Backward Force
Forward Force
1
2
Side-to-Side Force
2
3
Upward Force
3
Downward Force
4
Right Feet Force
4
5
Left Feet Force
5

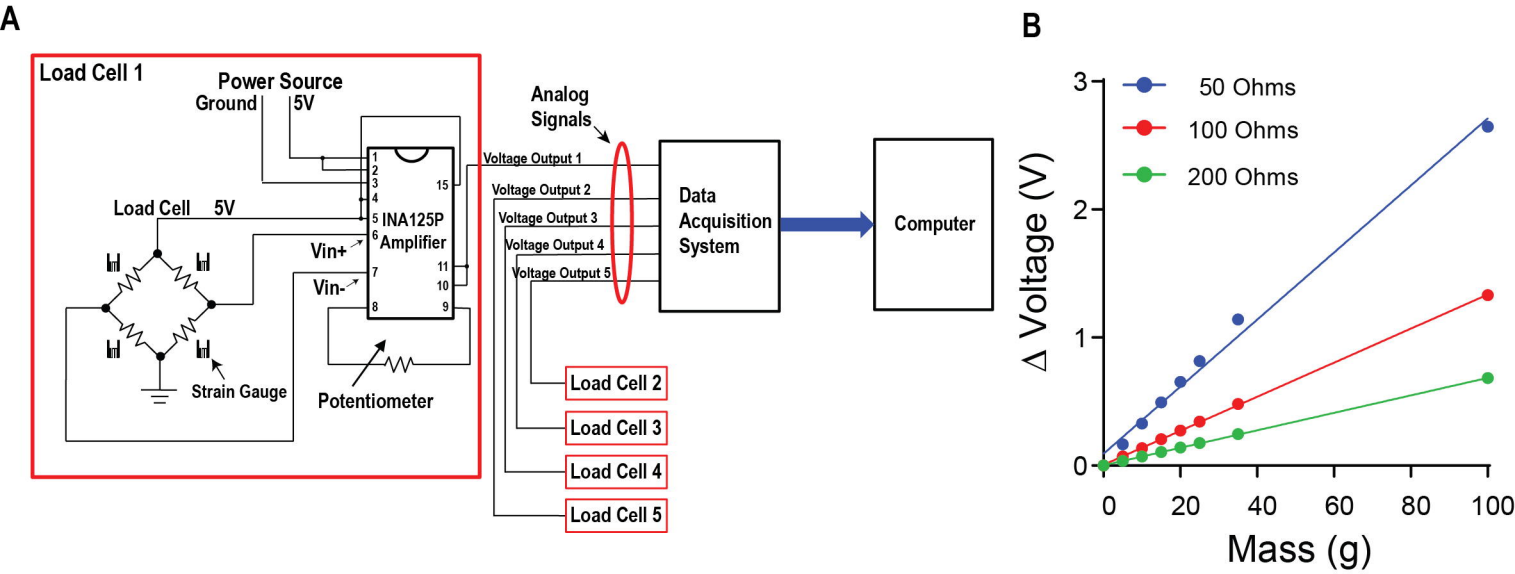
A
Load Cell 1
Power Source
Ground
5V
Load Cell
5V
INA125P
Amplifier
Vin+
Vin-
Strain Gauge
Potentiometer
Analog
Signals
Voltage Output 1
Voltage Output 2
Voltage Output 3
Voltage Output 4
Voltage Output 5
Data
Acquisition
System
Computer
Load Cell 2
Load Cell 3
Load Cell 4
Load Cell 5
B
50 Ohms
100 Ohms
200 Ohms
Δ Voltage (V)
Mass (g)
0
1
2
3
0
20
40
60
80
100

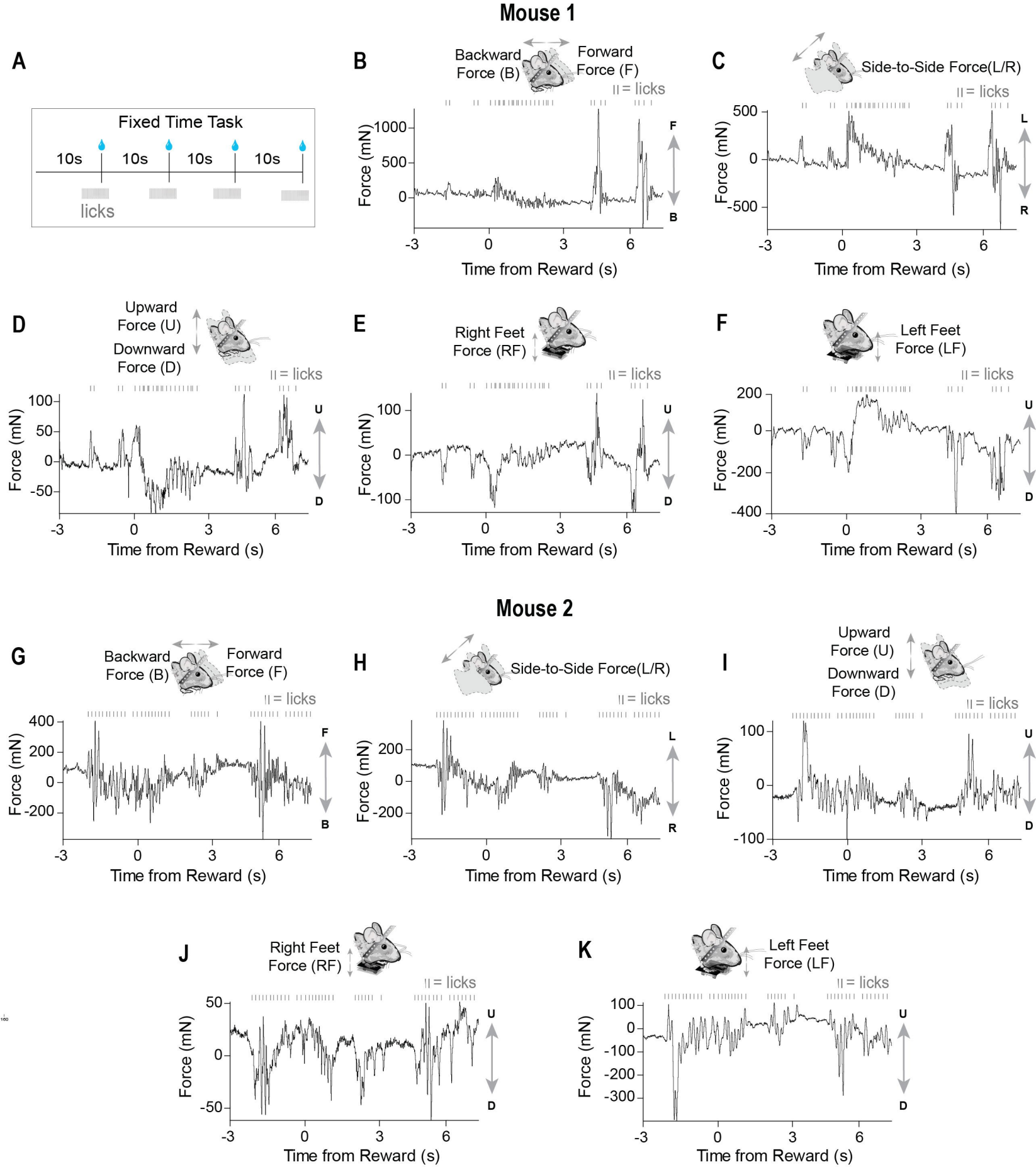
Mouse 1
A
Fixed Time Task
10s
10s
10s
10s
licks
B
Backward Force (B)
Forward Force (F)
|| = licks
Force (mN)
Time from Reward (s)
C
Side-to-Side Force(L/R)
|| = licks
Force (mN)
Time from Reward (s)
D
Upward Force (U)
Downward Force (D)
|| = licks
Force (mN)
Time from Reward (s)
E
Right Feet Force (RF)
|| = licks
Force (mN)
Time from Reward (s)
F
Left Feet Force (LF)
|| = licks
Force (mN)
Time from Reward (s)
Mouse 2
G
Backward Force (B)
Forward Force (F)
|| = licks
Force (mN)
Time from Reward (s)
H
Side-to-Side Force(L/R)
|| = licks
Force (mN)
Time from Reward (s)
I
Upward Force (U)
Downward Force (D)
|| = licks
Force (mN)
Time from Reward (s)
J
Right Feet Force (RF)
|| = licks
Force (mN)
Time from Reward (s)
K
Left Feet Force (LF)
|| = licks
Force (mN)
Time from Reward (s)

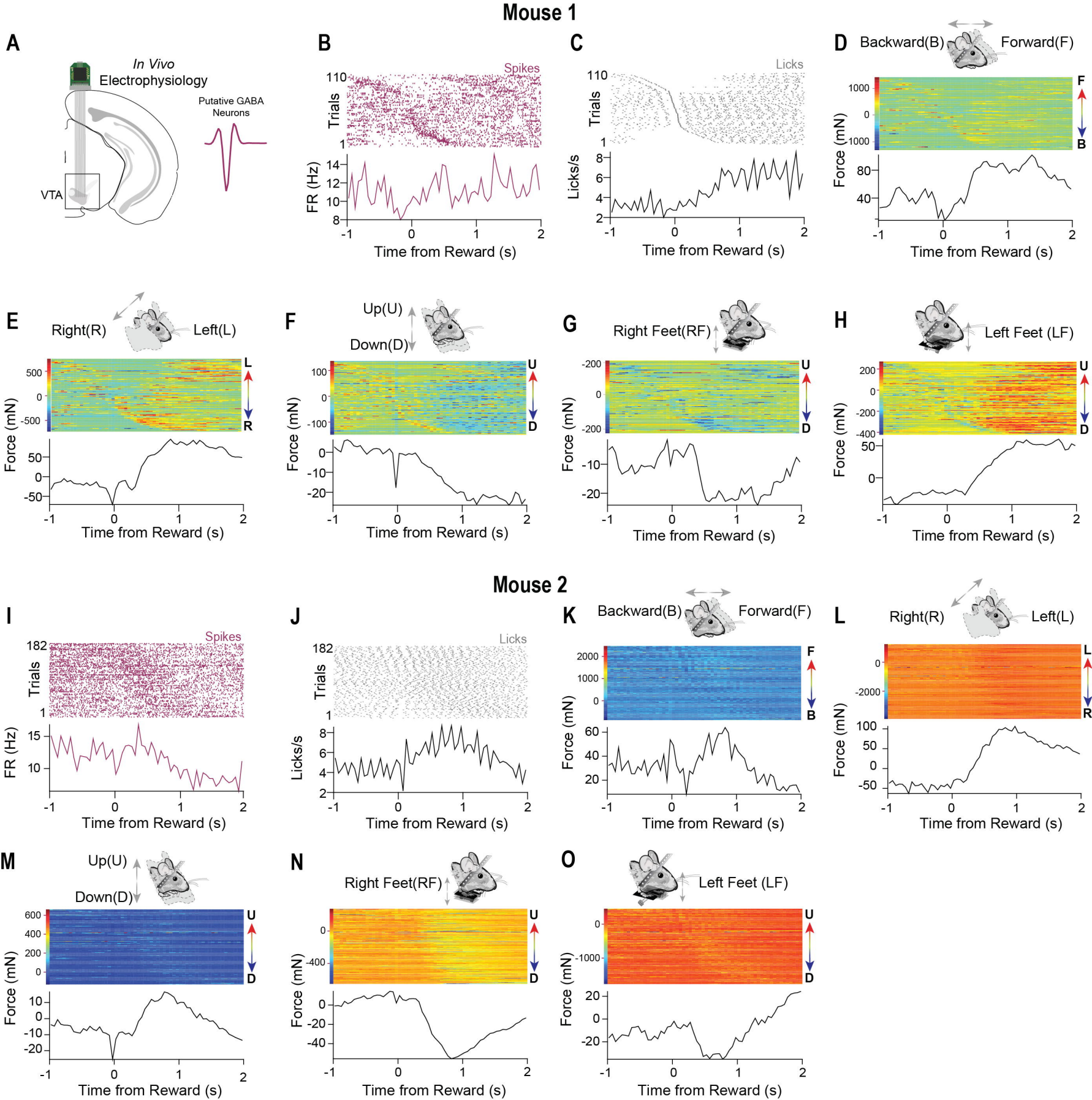
Mouse 1
A
In Vivo
Electrophysiology
Putative GABA
Neurons
VTA
B
Spikes
Trials
FR (Hz)
Time from Reward (s)
C
Licks
Trials
Licks/s
Time from Reward (s)
D
Backward(B)
Forward(F)
Force (mN)
Time from Reward (s)
E
Right(R)
Left(L)
Force (mN)
Time from Reward (s)
F
Up(U)
Down(D)
Force (mN)
Time from Reward (s)
G
Right Feet(RF)
Force (mN)
Time from Reward (s)
H
Left Feet (LF)
Force (mN)
Time from Reward (s)
Mouse 2
I
Spikes
Trials
FR (Hz)
Time from Reward (s)
J
Licks
Trials
Licks/s
Time from Reward (s)
K
Backward(B)
Forward(F)
Force (mN)
Time from Reward (s)
L
Right(R)
Left(L)
Force (mN)
Time from Reward (s)
M
Up(U)
Down(D)
Force (mN)
Time from Reward (s)
N
Right Feet(RF)
Force (mN)
Time from Reward (s)
O
Left Feet (LF)
Force (mN)
Time from Reward (s)

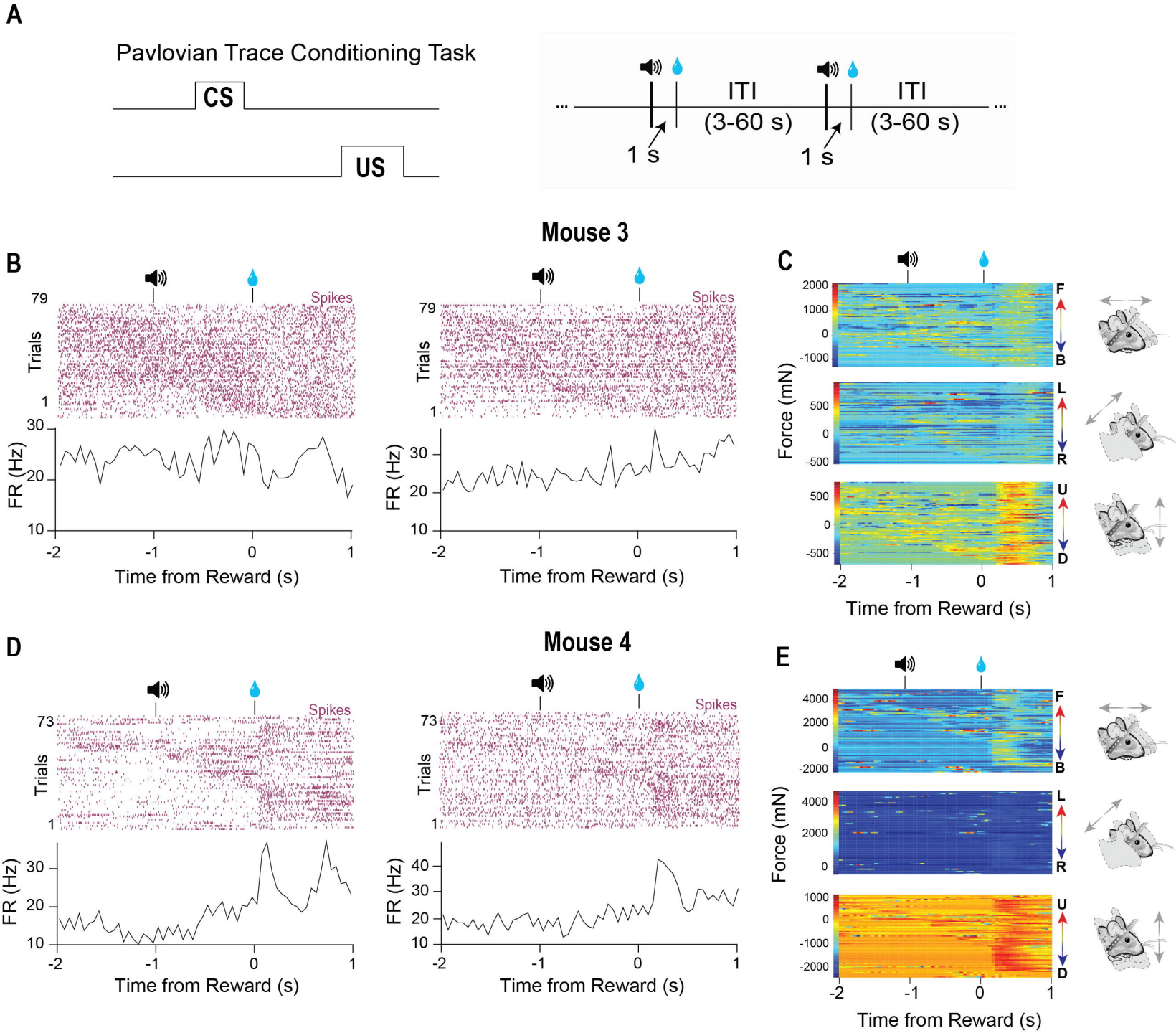
A
Pavlovian Trace Conditioning Task
CS
US
ITI
(3-60 s)
1 s
ITI
(3-60 s)
1 s
Mouse 3
B
Spikes
Trials
79
1
FR (Hz)
30
20
10
-2
-1
0
1
Time from Reward (s)
Spikes
Trials
79
1
FR (Hz)
30
20
10
-2
-1
0
1
Time from Reward (s)
C
Force (mN)
2000
1000
0
-1000
F
B
500
0
-500
L
R
500
0
-500
U
D
-2
-1
0
1
Time from Reward (s)
Mouse 4
D
Spikes
Trials
73
1
FR (Hz)
30
20
10
-2
-1
0
1
Time from Reward (s)
Spikes
Trials
73
1
FR (Hz)
40
30
20
10
-2
-1
0
1
Time from Reward (s)
E
Force (mN)
4000
2000
0
-2000
F
B
4000
2000
0
L
R
1000
0
-1000
-2000
U
D
-2
-1
0
1
Time from Reward (s)